(6) Matějka, L.; Dušek, K.; Dobáš, I. *Polym. Bull.* **1985**, *14*, 309.
(7) Reyx, D.; Costes, B.; Matějka, L.; Dušek, K. *Polym. Bull.* **1988**, *19*, 269.
(8) Attias, A. J.; Ancelle, J.; Bloch, B. *European Symposium on Polymeric Materials, Chemical Aspects in Processing Operations and use of Polymeric Materials*; Lyon, 1987; p CPA 08.
(9) Rozenberg, V. A. Epoxy Resins and Composites. *Adv. Polym. Sci.* **1986**, *75*, 113.
(10) Costes, B.; Reyx, D.; Platzer, N. *Makromol. Chem.* **1989**, *190*, 349.
(11) Attias, A. J.; Ancelle, J.; Bloch, B.; Laupretre, F. *Polym. Bull.* **1987**, *18*, 217.

Charge Storage on a Conducting Polymer in Solution

M. J. Nowak,[†,‡] D. Spiegel,[†] S. Hotta,[§] A. J. Heeger,*[,⊥] and P. A. Pincus[∥]

Institute for Polymers and Organic Solids, University of California, Santa Barbara, California 93106. *Received October 24, 1988; Revised Manuscript Received January 10, 1989*

ABSTRACT: Magnetic and optical studies of poly(3-hexylthienylene) (P3HT), doped in solution with $NO^+PF_6^-$ in both chloroform and in the more polar solvent methylene chloride (CH_2Cl_2), indicate a relatively small difference in the energy of polarons versus that of bipolarons and imply that the weak effective electron–electron Coulomb repulsion can be controlled by varying the solvent and/or the polymer concentration. As a result, we have observed unambiguous magnetic and optical signatures characteristic of polarons in P3HT in CH_2Cl_2 at the lowest doping levels. The relative fraction of polarons and bipolarons has been analyzed in the context of various proposed statistical models. A theoretical model is developed to include the effect (in such solutions) of ionic screening on the effective Coulomb interaction. This model is tested by adding salt to a dilute solution of doped polymer.

I. Introduction

In a nondegenerate ground state conjugated polymer such as polythiophene or its soluble alkyl derivates (Figure 1a), the fundamental nonlinear excitations and the dominant charge storage configurations are polarons and bipolarons.[1-4] The relative stability of these species depends on the relative strength of the electron–phonon and electron–electron interactions in the polymer. The doubly charged bipolaron is a bound state (resulting from the electron–phonon interaction) between two polarons. However, the repulsive Coulomb interaction favors the existence of two separated polarons. Hence, the energy of creation of two polarons may be comparable to that of a bipolaron.

In Figure 1b,c, we show the band diagrams with gap states and allowed optical transitions appropriate for a self-localized bipolaron and polaron, respectively.[1,3,4] Clearly, the two have distinguishing optical and magnetic signatures. A bipolaron with its two empty states in the gap carries a double-positive charge and is spinless. Two broad electronic transitions from the valence band to the gap states are expected with energies less than the interband transition. On the other hand, a polaron has one unpaired electron in its lower gap state, and hence, along with one positive charge, it has spin one-half. From Figure 1c, a polaron should display an additional subgap transition between two localized energy levels.

From these magnetic and spectroscopic signatures, studies of polythiophene and the poly(3-alkylthiophenes) have provided evidence that upon doping[1,6] or photoexcitation[7] charge is stored in spinless bipolarons. These results were obtained from measurements on the polymer in the form of solid-state films and powders and on the polymer in solution.[5-9]

There are reports by various groups,[10] however, that polarons are generated as well as bipolarons. This suggests a near degeneracy in the energy of two polarons versus a bipolaron, implying an equilibrium for the reaction

$$P^+ + P^+ \rightleftharpoons B^{2+}$$

Even in the case where bipolarons have the lowest creation energy, the entropy favors polarons so that a finite concentration of polarons can be expected. In this paper, we address this question with visible–near-IR spectroscopy and electron spin resonance data on the poly(3-hexylthienylene) system.[8,9]

The experimental results which we report here were carried out with poly(3-hexylthienylene) (P3HT) in a methylene chloride solution. By conducting the experiments in this more polar solvent than that used in previous work[9] (in chloroform), we find distinctly different behavior for the doped polymer in solution. For example, in the most dilute doping regime, our data indicate that charge storage is predominantly in polarons, in marked contrast with the low doping regime results of P3HT in chloroform. Only at higher doping levels in methylene chloride do we again observe the bipolaron as the dominant charge storage configuration. This implies an important solvent dependence to the polaron–bipolaron equilibrium described above.

By performing the experiments on a doped conducting polymer while it is in solution, it becomes possible to explore the effect of counterion screening on the interactions in the polymer. The effective on-chain Coulomb interaction between two polarons, although always repulsive, is strongly dependent on the extent to which the "bare" positive charge of the polaron is screened. To first order, this is determined by the proximity of its counterion. Second-order effects include the direct screening of the polarons by the solvent itself. This can be considered weak

[†] Department of Physics.
[‡] Current address: Bell Communications Research, Red Bank, NJ 07701-7020.
[§] Permanent address: Central Research Laboratories, Matsushita Electric Industrial Co., Ltd., Moriguchi, Osaka 570, Japan.
[⊥] Department of Physics and Engineering Materials Department.
[∥] Engineering Materials Department.

0024-9297/89/2222-2917$01.50/0 © 1989 American Chemical Society

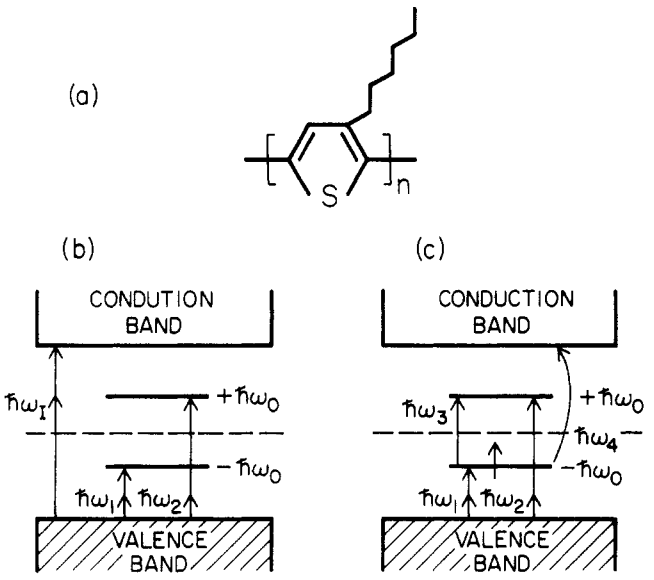

Figure 1. (a) Chemical structure of poly(3-hexylthienylene) (P3HT). (b) Band diagram showing the gap states and allowed transitions for a self-localized bipolaron. (c) Band diagram showing the gap states and allowed transitions for a self-localized polaron.

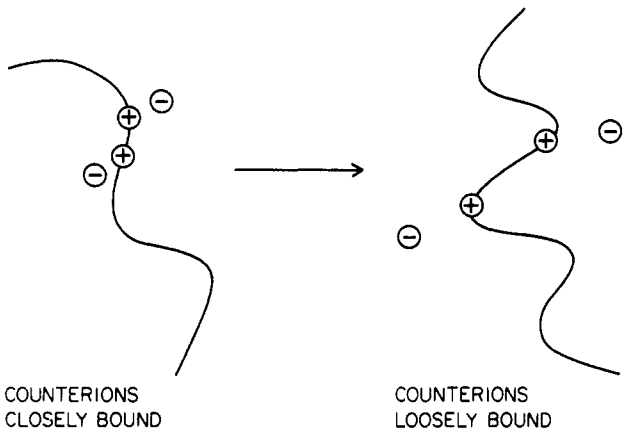

Figure 2. Schematic drawing of counterion screening of charged states on a conducting polymer in solution.

since even our "polar" solvent, methylene chloride, is only weakly polar (compared, for example, to water).

Illustrated in Figure 2 are two possible limits. If, as in a nonpolar solvent, the counterions are closely bound to the polarons on a chain, the *net* polaron–polaron interaction due to the electron–phonon interaction can be attractive. In a more ionic environment, such as a polar solvent, the counterions are more loosely bound to the chains. With a larger separation between charges in the π-system and counterion, the *net* polaron–polaron interaction becomes more repulsive. To some extent, then, it is possible to control the relative energies of the doubly charged bipolaron in comparison to two singly charged polarons. In this study of P3HT in solution, the strength of the counterion screening has been altered by varying the solvent, the polymer concentration, or the salt concentration of a conducting polymer solution.

II. Experimental Section

Details of the preparation and characterization of the polymer can be found elsewhere.[8,9] The soluble P3ATs have a relatively high molecular weight (≈300 monomer units) and high purity. Infrared studies have characterized these materials as 2,5-linked linear polythienylene chains. Solutions were prepared by dissolving P3HT in methylene chloride; all samples were prepared under a dry nitrogen atmosphere. The dopant ($NOPF_6$) was purified by sublimation at ca. 125 °C under a reduced pressure of $\approx 2 \times 10^{-3}$ Torr and then dissolved in acetonitrile. Both the dichloromethane and acetonitrile were dried and distilled over phosphorus pentoxide under dry nitrogen. Doped polymer solutions were prepared by adding the appropriate amount of the dopant solution (4 mg of $NOPF_6$ in 1 mL of acetonitrile) to previously prepared dichloromethane solutions of P3HT. The quoted y values are nominal and assume that the doping reaction has gone to completion with each NO^+ ion, yielding a transfer of one electron from a P3HT macromolecule. In chloroform, the doping of P3HT was strongly dependent on the polymer concentration and, consequently, all samples were doped at high polymer concentrations where the doping was more efficient and then diluted.[9a] The doping of the dichloromethane solution was efficient and exhibited only a very weak polymer concentration dependence.

Volumetrically accurate amounts of solutions were sealed in optical cells or in ESR tubes to ensure against loss of volatile solvents during the measurements. Although we observed no obvious signs of degradation or instability, all of our studies routinely utilized freshly prepared samples. The solutions of both the neutral polymer and the doped polymer were clear and stable over long times with no indication of cloudiness, aggregation, or precipitation. For example, doped CH_2Cl_2 solutions were extraordinarily stable for periods of more than a month. Therefore, P3HT exists as a macromolecular chain in solution both when neutral and when partially oxidized by doping. Quasi-elastic light scattering from neutral polymer solutions yields a hydrodynamic diameter of ≈300 Å.[11] Since the mean molecular weight[9] corresponds to approximately 300 monomer units, this implies the polymer is a wormlike chain in solution. The dilute regime (mean separation between chains is greater than the hydrodynamic diameter) is therefore restricted to polymer concentrations of $c \leq c_0 = 1$ mg/mL, or approximately 6×10^{-3} M. For $c \geq c_0$, interchain interactions become important. Doping experiments were carried out at a polymer concentration of about c_0, the best compromise for high signal intensity without significant interchain interactions.

Magnetic resonance measurements were performed on an IBM Instruments Bruker 200D electron spin resonance spectrometer interfaced with an Apple IIe computer for data acquisition and analysis. The visible–IR absorption spectrum was obtained with a McPherson EU700 monochromator and either a photomultiplier or an IR Industries Si/PbS two-color detector using standard light chopping and lock-in amplifier techniques. The monochromator grating drive and detector electrons were interfaced to an IBM PCXT which collected and stored the data. In order to obtain the optical density of P3HT alone, the optical spectrum of the pure solvent was subtracted from the spectrum of the polymer solution.

III. Data

III.A. Electron Spin Resonance Measurements.

Previous studies[9a] of P3HT in a chloroform solution indicate a strong dependence of the magnetic susceptibility on the polymer concentration. In a methylene chloride solution, on the other hand, the susceptibility is independent of the polymer concentration. In "nonpolar" chloroform (dielectric constant = 4.73), ionic screening caused by neighboring polymer chains becomes important at concentrations near or greater than the overlap concentration c_0; in effect, the medium becomes more polar due to the dissolved polyelectrolyte and anions. As discussed above, a polar solvent will lead to a counterion separation and thereby to a shift in the equilibrium toward a greater fraction of polarons. With a more polar solvent such as methylene chloride (dielectric constant = 9.73), an increase in polymer concentration would be expected to have a small effect on the ionic strength of the doped polymer solution.

Figure 3 shows the dependence of the magnetic susceptibility on the nominal doping level y at a fixed polymer concentration of $c = c_0$ in methylene chloride. In the pristine polymer, a susceptibility corresponding to one spin

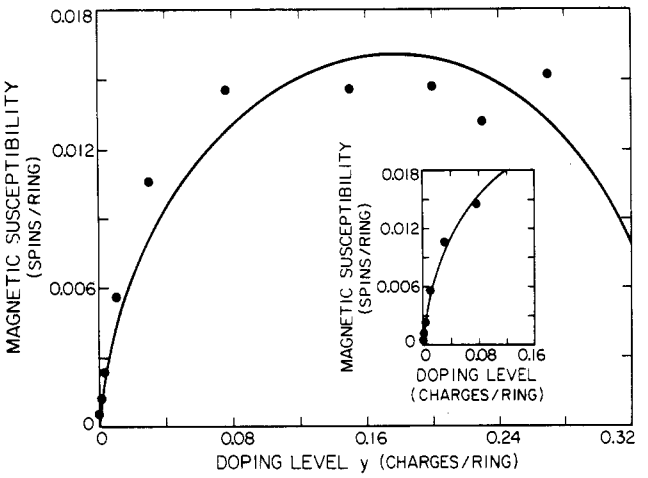

Figure 3. Magnetic susceptibility versus dopant level at a fixed polymer concentration $c = c_0$ in dichloromethane. The solid line is the best fit given by the bead model with $\eta = 582$ ($\Delta = 0.16$ eV) and $p = 2.94$. Inset: The initial behavior is reproduced with $\eta = 400$ ($\Delta = 0.15$ eV).

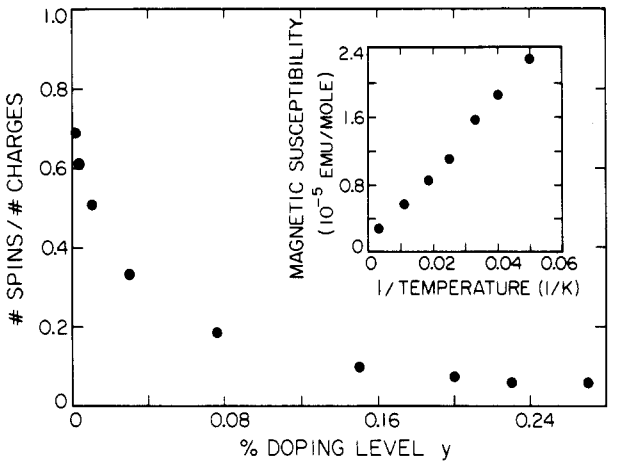

Figure 4. Ratio of spins to charge versus dopant level at a fixed polymer concentration $c = c_0$ in dichloromethane. The number of spins in the figure is the number of additional spins upon doping; i.e., the background (pristine) signal has been subtracted away. Inset: Temperature dependence of P3HT in CH_2Cl_2 with $c = c_0$ and $y = 0.3\%$.

per 1000 rings is understood to originate from defects on the polymer chains. The susceptibility initially increases rapidly with dopant concentration, but saturates at one spin per 60 rings.

The strong dependence of the number of spins per charge on the amount of charge injected can be more dramatically displayed by plotting the ratio of spins per charge as a function of doping level, as in Figure 4. In this figure, we include only the number of additional spins in the solution; i.e., the background (pristine) signal has been subtracted away. Because of the fundamentally different spin/charge relationships exhibited by polarons versus bipolarons, the spin-to-charge ratio plotted in this curve can be thought of as a direct indication of the relative fraction of polarons in the material (the remainder of the charge being stored in bipolarons). In this context, note that at the highest doping levels, one spin is present for approximately 20 charges deposited on the polymer chains, strongly indicating that bipolarons are the dominant charge storage state in this regime. At low doping levels, however, this is clearly not the case. At the lowest doping level, the ratio approaches the value of 1.0, indicating that charge is stored in the self-localized states associated with polarons. This is consistent with the predictions of various

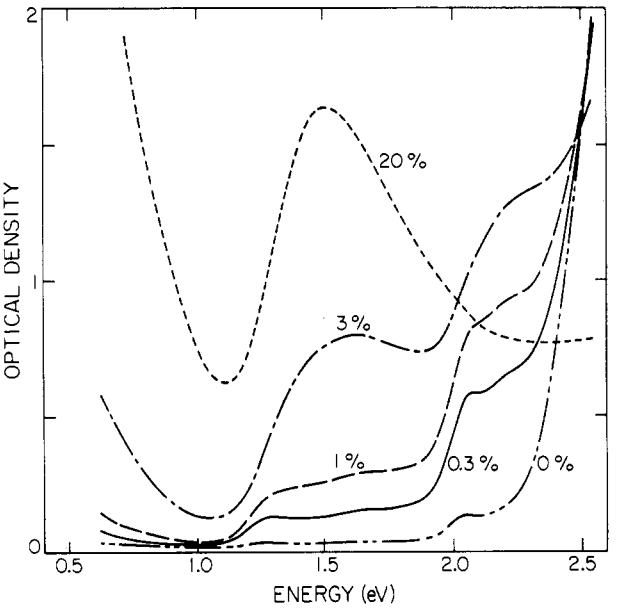

Figure 5. Optical absorption spectra of P3HT in CH_2Cl_2 at $c = c_0$ at various doping levels: $y = 0\%$, 0.3%, 1.0%, 3.0%, and 20%. The residual structure in the spectrum labeled as 0% indicates the presence of residual dopant (<0.1%) remaining from the original electrochemical synthesis.

statistical calculations which show that although the bipolaron is energetically favored, entropy favors the polaron, particularly at the most dilute concentrations. In the low-y regime, the temperature dependence of the magnetic susceptibility in the range 20–300 K is shown in Figure 4 (inset). The magnetic susceptibility of the solution, frozen throughout most of the measurement, exhibits a Curie law characteristic of a localized paramagnetic spin.

III.B. Spectroscopic Measurements. Most of the optical work was completed by using a polymer concentration of $c \approx c_0$. The spectra at various doping levels were also measured at lower concentrations; no significant changes in the absorption spectrum were observed. Figure 5 shows spectra obtained at different doping levels (y). For the neutral polymer, the interband transition is seen to have a threshold at approximately 2.2–2.3 eV. Upon doping at dilute levels ($y \leq 1\%$), we note considerable fine structure; one observes a defined peak at $\hbar\omega = 2.05$ eV and broad but discernible peaks at the energies of 1.2, 1.6, and 2.2 eV along with the trailing edge of an infrared feature. Using Fourier transform infrared interferometry, we have found a broad absorption band at about 0.4–0.5 eV (although the FTIR results are complicated by strong solvent absorption lines in this spectral region). As the doping level is increased, the subgap absorptions grow at the expense of the interband transition. These features broaden and overlap such that at high doping levels ($y \approx 0.20$) there is a broad peak at 1.5 eV accompanied by the rising edge of a second absorption in the infrared, peaked at approximately 0.6 eV (as inferred from FTIR studies). Consistent with the sum rule, all the oscillator strength associated with the interband transition has been shifted to two broad peaks below the gap.

The higher dopant level data are consistent with previously reported optical spectra of heavily doped polythiophenes and their derivatives.[6-9] At $y = 20\%$, we see oscillator strength as shifted away from the higher energy (2.05 eV and interband) transitions into the two lower energy gap states. These correspond to the possible absorptions for a bipolaron shown in Figure 1b and suggest that at high doping levels charge is predominantly stored in bipolarons. This is fully consistent with the magnetic

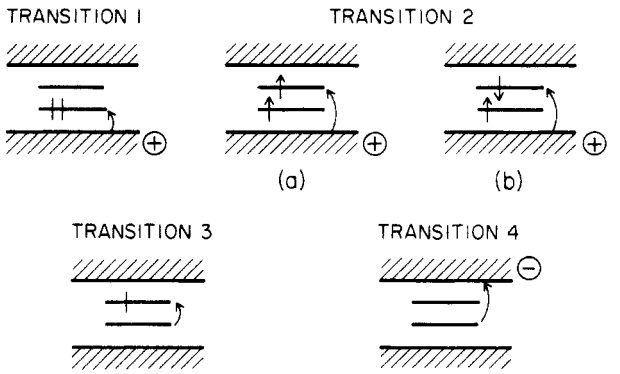

Figure 6. Final states of optical transitions expected for a positive, singly charged polaron state.

resonance results which indicate that at $y \approx 0.2$, only approximately 5% of the charge is stored in polarons with the remainder in spinless bipolarons.

It is possible to estimate the strength of the Coulomb interaction in this high doping regime by substituting these values in the relation[6b,7,9]

$$\hbar\omega_1 + \hbar\omega_2 = E_g - 2(U_B - E_B) \quad (1)$$

where $2U_B$ is the difference in Coulomb energy between a singly and a doubly charged state and $2E_B$ is the binding energy of the counterion. Because of the counterion term, it is impossible to calculate the strength of the diagonal Coulomb integrals directly. From the data of Figure 5, we estimate $U_B - E_B \approx 0.1$ eV, suggesting that Coulomb energies on a polymer are roughly comparable to the energy of interaction of the self-localized charges states on the polymer with their associated counterions.

The gap states (see Figure 1b) associated with the bipolarons are located at approximately 0.6 and 1.5 eV above the valence band. This is in relatively close agreement with the values (0.34 and 1.67 eV) obtained by Bredas et al.[12] using a generalized SSH model[2b] (tight binding band structure plus σ-compressibility). The relatively small shifts between experiment and theory are consistent with relatively weak electron–electron Coulomb interactions, even for P3HT in dilute solution.

At the lowest doing levels (below 1%) the magnetic data summarized in the previous section indicate that charge is stored predominantly in the form of self-localized charged polarons. Thus, the complex spectrum evident in Figure 5 at these doping levels must be understood in the context of polarons. Based on the energy level structure of Figure 1c, one would expect no more than three transitions. Figure 6 shows (in more detail) the optical transitions expected for a positive, singly charged polaron state.[1] There are in addition to the interband transition $\hbar\omega_1 = E_g$ (where E_g is the band gap) four transitions which either add an electron or hole to the polaronic state. The energy levels depicted in Figure 1 and 6 represent single-particle eigenenergies and, as such, do not include any effects due to Coulomb repulsion. In the absence of Coulomb interactions, and given electron-hole symmetry, it is obvious that

$$\omega_2 = \omega_4 \quad (2)$$

and

$$\omega_1 + \omega_3 = \omega_4 \quad (3)$$

Including on-site and nearest-neighbor Coulomb interactions in an extended Hubbard model,[13] one finds that transition 1 is not shifted. Transitions 2a and 2b have final states which are identical except for spin considerations; two electrons localized on the polaron may, in general, form either a triplet or singlet two-particle state. Therefore, we expect the transition energy, $\hbar\omega_2$, to be split into a doublet when Coulomb energies are important. Transition 3 between localized levels in the gap (with no change in the charge on the polaron) is unaffected by the Coulomb interaction. Transition 4 exhibits a double-charged final state in which the Coulomb repulsion characteristic of a bipolaron will be important.

Although it is tempting to assign the multiple peaks for dilute concentrations in Figure 5 to the many allowed transitions sketched in Figure 6, the excellent agreement of the bipolaron spectrum with that predicted by Figure 1b implies that the electron–electron Coulomb interactions are weak and hence that the splittings alluded to above are small. Therefore we use the results calculated[12] for polarons in the absence of Coulomb repulsion as a guide. For weak electron–electron interactions, Bredas et al.[12] predict three peaks in polythiophene; at 0.5, 1.1, and 1.6 eV. These correspond nicely to the spectral features observed in Figure 5 (at low doping): a peak below 0.5 eV and two peaks at ~1.2 and ~1.6 eV, respectively.

With these assignments (based upon theory and consistency with the bipolaron spectra at higher doping levels), the relatively sharp peak at 2.05 eV and the weaker feature at ~2.2 eV are unexplained. A similar weak feature was observed in spectroscopic studies of doped P3HT in chloroform.[9a] As noted in earlier studies,[9] there is a blue shift of the π–π^* transition for P3HT in solution as compared with either films or macromolecular aggregates. The straight-chain conformation characteristic of the solid state has a π–π^* transition that onsets at ≈1.9 eV, whereas in dilute solution, the onset is at ≈2.2 eV. Moreover, experimental evidence and calculations (in the context of the conformon model[14]) imply that the straight-chain conformation is restored in the vicinity of a polaron or bipolaron.[9a] Since the persistence length is expected to be quite long,[15,16] at dilute concentrations such straight sections may well extend beyond the region of the polaron distortion. Thus the structure at $\hbar\omega$ near 2.0–2.2 eV may arise from interband contributions from these locally straight-chain regions, rather than from gap states associated with the self-localized polarons.

IV. Analysis of the Magnetic and Spectroscopic Data: The Statistics of Polarons and Bipolarons

As noted in the Introduction, the competition of the indirect attraction between two polarons via the self-consistent structural distortion and their Coulomb repulsion leads to a near degeneracy in the energy of two polarons versus that of a bipolaron, implying an equilibrium in the reaction

$$P^+ + P^+ \rightleftharpoons B^{2+}$$

Even in the case where bipolarons have the lowest creation energy, the entropy favors polarons (there are more statistically independent configurations for two polarons each with two possible spin degrees of freedom than for a single spinless bipolaron), so that a finite concentration of polarons can be expected, particularly at low doping concentrations and at relatively high polymer concentrations. In this section we explore the statistics of a system of polarons and bipolarons by analyzing two simple models with the goal of obtaining the free energy and, thereby, the concentrations of the two species as a function of the doping level. We examine the different models, each successful to some degree, in order to gain insight into the important features that determine the equilibrium between polarons and bipolarons.

IV.A. The Bead Model. Let us first consider a simple model of the statistical mechanics of polarons and bipolarons on a chain.[17] The configurational entropy of placing P polarons and B bipolarons on a polythiophene chain is an important component of the free energy. Given a chain of N sites, it is possible to derive an expression for the total number of configurations in the continuum limit ($1 \ll B$, $P < N$) by considering the polarons and bipolarons to be solid beads on a ring (periodic boundary conditions). The number of configurations for P beads of length pa and for B beads of length ba on a ring of circumference Na (where a is the lattice spacing) is the sum (or integral) of the possible configurations of each of the beads, i.e.

$$\Omega_1 = \int_{\substack{\text{bead} \\ P+B}} \cdots \int_{\substack{\text{bead} \\ 1}} \frac{dx_1}{a} \cdots \frac{dx_{P+B}}{a} \tag{4}$$

where x_i is the position of the ith bead. As will become evident, one need not distinguish between polarons and bipolarons at this stage of the calculation. The first bead (a polaron in this case) can be placed from the origin, 0, to the end of the second bead x_2 (less one polaronic bead length pa). Then

$$\int_0^{x_2-pa} \frac{dx_1}{a} = \left(\frac{x_2 - pa}{a}\right) \Big/ 1! \tag{5}$$

If the next bead is a bipolaron, then

$$\int_{pa}^{x_3-ba} \frac{x_2 - pa}{a} \frac{dx_2}{a} = \frac{\left(\dfrac{x_3 - pa - ba}{a}\right)^2}{2!} \tag{6}$$

and so on

$$\int_{pa+ba}^{x_4-pa} \frac{\left(\dfrac{x_3 - pa - ba}{a}\right)^2}{2!} \frac{dx_3}{a} = \frac{\left(\dfrac{x_4 - 2pa - ba}{a}\right)^3}{3!} \tag{7}$$

etc. Hence, the final integral has the following form

$$\Omega_1 = \int_{Bba+(P-1)pa}^{Na-Pa} \frac{\left(\dfrac{x_{P+B} - Bba + (P-1)pa}{a}\right)^{(B+P-1)} \dfrac{dx_{P+B}}{a}}{(B + P - 1)!} \tag{8}$$

which yields

$$\Omega_1 = \frac{(N - Bb - Pp)^{(P+B)}}{(P + B)!} \tag{9}$$

This is the number of configurations for P polarons and B bipolarons on a ring of N sites but for only one distinguishable sequence, for example, BBPPBPPP ... etc. To account for all the distinguishable ways to put P polarons and B bipolarons on a ring, a multiplicative factor must be introduced:

$$\Omega = \Omega_1 \left(\frac{P + B}{P}\right) \tag{10}$$

which yields

$$\Omega = \frac{(N - B - Pp)^{(P+B)}}{B!P!} \tag{11}$$

This is the total number of configurations for P polarons and B bipolarons on a ring of N sites.

Now it is possible to calculate the free energy for P polarons and B bipolarons on a ring corresponding to a polythiophene chain. Denote by E_p the energetic cost of adding a polaron to a chain of polythiophene rings, corresponding to the oxidation reaction

$$PT^0 \rightarrow P^+ + e^- \tag{12}$$

Similarly let E_B denote the energetic cost of adding a bipolaron to the system, corresponding to the reaction

$$PT^0 \rightarrow B^{2} + 2e^- \tag{13}$$

Given these definitions, the Helmholtz free energy of a system containing P polarons and B bipolarons is

$$F = PE_p + BE_B - kT \ln \Omega - kTP \ln 2 \tag{14}$$

The last term is due to the spin degree of freedom of the polarons. This free energy determines the equilibrium chemical potentials μ_P and μ_B for polarons and bipolarons, respectively. Making use of Stirling's approximation for $\ln (x!)$, straightforward differentiation yields

$$\mu_P \equiv (\partial F/\partial P)_B \approx E_P - kT \ln (N - Pp - Bb) + \frac{kT(P + B)p}{N - Pp - Bb} + kT \ln P - kT \ln 2 \tag{15}$$

and

$$\mu_B \equiv (\partial F/\partial B)_P \approx E_B - kT \ln (N - Pp - Bb) + \frac{kT(P + B)b}{N - Pp + Bb} + kT \ln B \tag{16}$$

According to the theory of chemical equilibrium, $\mu_B = 2\mu_P$. Hence, a second equation of μ_P can be obtained by writing

$$\mu_P = \mu_B - \mu_P$$

i.e.

$$\mu_P = (E_B - E_P) + \frac{kT(B + P)(b - p)}{N + Pp - Bb} + kT \ln \left[\frac{2B}{P}\right] \tag{17}$$

An expression for the system's equilibrium polaron concentration as a function of temperature and the amount of injected charge can now be derived by combining the two equations for μ_p and using the law of charge conservation $Q = P + 2B$. With Δ defined as the difference in energy between polarons and bipolarons

$$\Delta = 2E_p - E_B \tag{18}$$

the combined equations yield the relation

$$kT \ln \left[\frac{4B(N - Pp - Bb)}{P^2}\right] = \Delta + \frac{kT(B + P)(2p - b)}{N - Pp - Bb} \tag{19}$$

The last term in this equation is negligible in the low-density limit where the concentration of injected charges is still dilute. Defining the variable

$$\eta \equiv e^{\Delta/kT}$$

our expression becomes

$$\eta = \frac{4B(N - Pp - Bb)}{P^2} \tag{20}$$

With the relation $B = (Q + P)/2$, this yields a quadratic equation for the polaron concentration P. If we assume

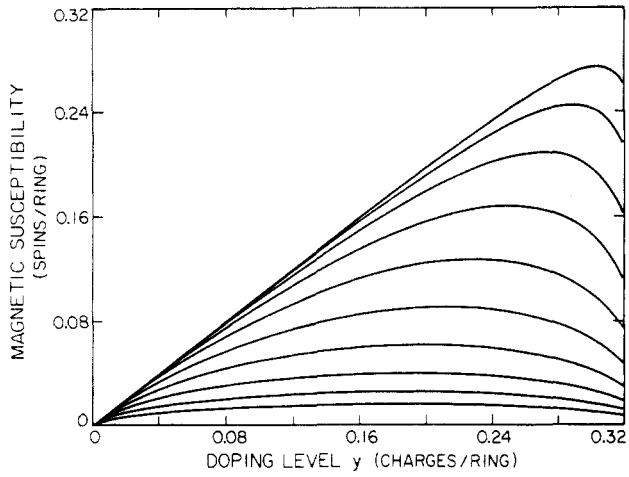

Figure 7. Series of plots of the polaron concentration P as a function of the injected charge Q for different values of the parameter η in the bead model. Beginning with the lowest curve: η = 592, 220, 80, 29.6, 10.8, 4.0, 1.48, 0.56, 0.20, and 0.072.

$2p \approx b$ (see ref 18 and the discussion in the following paragraphs), this equation is greatly simplified to

$$\mathcal{P} = \frac{1}{\eta}[[(\mathcal{Q}p - 1)^2 + 2\eta\mathcal{Q}(1 - \mathcal{Q}p)]^{1/2} + (\mathcal{Q}p - 1)] \quad (21)$$

where $\mathcal{P} = P/N$ and $\mathcal{Q} = Q/N$.

Figure 7 shows a series of plots of the calculated polaron concentration as a function of the injected charge Q for different values of the parameter η. For any positive value of the parameter Δ (bipolaron formation energetically favorable over two polarons), this curve exhibits a maximum whose height and position depend on the magnitude of Δ and the temperature. This demonstrates the essential point that the extra entropy of two polarons over a single bipolaron always permits a nonzero concentration of polarons. As bipolaron formation becomes increasingly favorable (Δ becomes arbitrarily large), the maximum polaron concentration becomes very small. All curves exhibit an initial linear regime that quickly yields a square root behavior, which, as will be shown, dominates the intermediate doping regime in our data. At sufficiently high doping levels, the polaron concentration saturates and eventually begins to decline. Finally, if bipolarons are not energetically favored over polarons (Δ zero or negative), the polaron concentration linearly increases as a function of the injected charge for all practical doping levels, i.e., those below the half-filled case.

Included in Figure 3 is a plot of the calculated polaron concentration as a function of the injected charge Q in direct comparison with the experimental data. A best fit of the data suggests that the polaron width is approximately three thiophene rings (having fixed the bipolaron width to be approximately twice the polaron width) and yields $\Delta \approx 0.16$ eV; i.e., bipolarons are indeed energetically favored over polarons. The statistics of the model ignore any interaction between polarons and bipolarons (e.g., polaron–bipolaron Coulomb repulsion) except for recombination. The plateau in the magnetic susceptibility versus doping level above 10% may imply such an interspecies interaction. An excellent fit for the data below 10% may be obtained (Figure 3, Inset), yielding approximately the same Δ of 0.15 eV.

Hartree–Fock semiempirical optimizations[18] of the geometry of polarons and bipolarons on a polythiophene chain indicate defect widths of about four rings for the polaron and six rings for the bipolaron, in good agreement with our estimates.

The essential difference between the bead model and a previously proposed box model[10] is the enumeration of the total number of possible configurations of polarons and bipolarons. In a box model, a polymer chain is broken into a collection of boxes into which one can place the charge storage species. In the bead model, a charged species is allowed to move all over the chain in a continuous fashion, subject only to the restriction that it not pass through other "beads" on the chain. The failure to account for this "positional" entropy may be responsible for a poorer fit of the data with a box model. Nevertheless, both models yield bipolarons as the lowest energy charge storage configuration. It is apparent, however, that the bead model more accurately reflects the entropic contribution to the free energy in the real system. Simple Hückel calculations[12] (including a σ-compressibility term) have been carried out for the energetics of polarons and bipolarons in polythiophene. The results indicate that a bipolaron is favored over two polarons by 0.26 eV. On the basis of the value $\Delta \approx 0.15$–0.16 eV, obtained from analysis of the experimental results, we conclude that the electron–electron interactions (which are not explicitly included in the Hückel calculations and which favor singly charged polarons with respect to doubly charged bipolarons) reduce the energy difference by about 0.1 eV.

It is also possible to understand the initial behavior of the magnetic susceptibility in terms of the conformon model.[14] Simply by studying the competition between the π-electron delocalization energy and chain conformation entropy of a conjugated polymer in solution, it is predicted that locally rigid regions containing one or more π-electrons are stable. Given a chain of N repeat units and an electron density of c on a chain, the number of conformons P is

$$P \approx N(\sigma c)^{1/2} \quad (22)$$

where σ is the statistical weight for creating a conformon.

Naively assuming half of the total number of "conformons" has an odd number of electrons and consequently exhibits a spin, one finds a susceptibility that depends on the concentration of electrons c (corresponding to charge injected) as $c^{1/2}$. This square root dependence is characteristic of bimolecular kinetics were linear aggregates can form from smaller species and is inherent in both the bead and box models at low doping levels (see eq 21).

IV.B. The Attractive Hubbard Model. One can reproduce the functional dependence of the polaron concentration on the doping level with a simple Hubbard model[19,20] (in the atomic limit) with an attractive on-site interaction U for two electrons. We calculate both the equilibrium polaron population and the concentration of electrons by varying the chemical potential. Whereas the bead model calculations was done with the canonical ensemble, in this calculation we use the formalism of the grand canonical ensemble.

Consider a one-dimensional lattice of N sites filled with n electrons and a Hamiltonian:

$$H = \sum_i [\epsilon n_i - U n_{i\uparrow} n_{i\downarrow}] \quad (23)$$

where ϵ is the energy of an electrons on a site, n_i is the number of electrons on site i, and U is the magnitude of the attractive on-site interaction between electrons with spin up ($\uparrow$) and electrons with spin down ($\downarrow$). We define the site energy of an empty site as zero. The hopping term t is set to zero in the localized "molecular" limit.

By simply calculating the grand partition function and the appropriate derivatives, one can derive expressions for the average number of unpaired electrons (polarons) and

for the average filling (Q, the amount of charge injected). Let μ' denote the chemical potential with $\beta = 1/kT$, then

$$z = \mathrm{Tr}\, e^{-\beta(H-\mu' N_i)} = 1 + 2e^{-\beta(\epsilon-\mu')} + e^{-\beta(2\epsilon-U-2\mu')} \quad (24)$$

Redefining the chemical potential as $\mu = \mu' - \epsilon$, the expression reduces to

$$z = 1 + 2e^{\beta\mu} + e^{\beta(U+2\mu)} \quad (25)$$

The doping level y is then calculated as the average number of electrons in the system divided by the total number of sites, N:

$$\langle n \rangle = \frac{1}{z\beta}\frac{\partial z}{\partial \mu} \approx y \quad (26)$$

and $y = \langle n \rangle / N$. Denoting B as the number of paired elecrons, i.e., those electrons in any doubly occupied sites

$$B = \frac{1}{z\beta}\frac{\partial z}{\partial U} = \frac{e^{\beta(U+2\mu)}}{z} \quad (27)$$

In this picture, the spinless, paired electrons bound to each other on one site can be thought of as the equivalent of bipolarons. It is then possible, by charge conservation, to calculate the number of singly occupied sites P:

$$P = \langle n \rangle - 2B = 2e^{\beta\mu}/z \quad (28)$$

A singly occupied site with its unpaired electron can be identified as the equivalent of a polaron. In other words, a singly occupied site would exhibit a magnetic susceptibility.

It is possible to rewrite eq 28 in a form reminiscent of the square root dependence of the polaron concentration on the amount of charge injected found in the previous models. Let us define

$$A(\mu,U) = ze^{\beta U}/2 \quad (29)$$

Charge conservation then yields the following quadratic equation:

$$Q = P + 2B = P + AP^2 \quad (30)$$

with the solution

$$P = \frac{-1 + (1 + 4Ay)^{1/2}}{2A} \quad (31)$$

Note that in the very small y limit, the polaron concentration $P \approx y$; i.e., the initial doping regime is linear. Only when the doping level becomes sufficiently large does a crossover to square root behavior occur. In Figure 8, we see numerically generated curves of P versus y for an attractive on-site interaction U of 0.20 and 0.21 eV. Note this curve is symmetric and reaches a maximum about $\langle n \rangle / N = y = 1$, as expected. For this concentration, we must have $\mu = -U/2$. Plotted alongside is the magnetic susceptibility versus doping level data of Figure 3. The observed magnitude of the maximum of P fixes A in the half-filled case to a value consistent with that derived from eq 29. The abcissa is multiplied by a factor of 6 in the experimental data in order to match the theoretically generated curves above. In this way, we identify one site with the approximate physical extent of a bipolaron, i.e., six rings.

The favorable fit suggests that, in this simplified picture, an attractive pairing interaction between electrons (or holes) and localization over approximately six thiophene rings are all that are necessary to interpret the data. This model predicts that bipolarons are favored over polarons by ≈0.2 eV, comparable to the more rigorously derived results presented above. This conclusion is consistent with previous work on polythiophene systems in the solid state,[5-7] where bipolarons are also found to be favored.

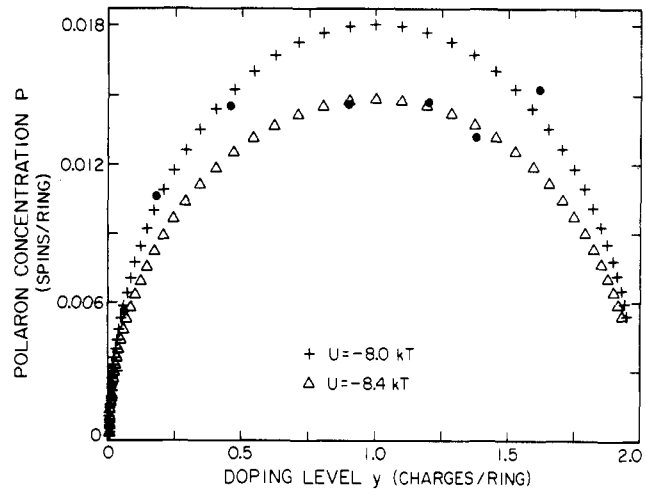

Figure 8. Magnetic susceptibility data of Figure 3 is plotted along with curves generated by a simple Hubbard model with only an on-site attractive interaction of U = 0.20 and 0.21 eV. The ordinate is the number of unpaired electrons per site and the abcissa is the average number of electrons per site. The experimental data are plotted as if one site is equivalent to six P3HT rings.

V. Discussion

V.A. The Role of Ionic Screening. In previous work on P3HT in solution in chloroform,[8] it was concluded that bipolarons (rather than polarons) were the most energetically favored charge storage configuration. This was based on the following understanding[8] of the strong polymer concentration dependence at a fixed doping level (see Figure 10). At low polymer concentrations ($c \ll c_0$; i.e. essentially no polymer–polymer interaction), the number of spins per charge drops to a negligible value (statistically half of the polymer chains have an odd number of charges and thus are forced to support a polaron; hence ~1 polaron per 600 thiophene rings is a minimum). This implies that the energetics of an isolated doped polymer chain in chloroform solution favors the spinless bipolarons. At high polymer concentrations ($c = c_0$), bipolarons are still dominant, four out of five charges are still in bipolarons, although the equilibrium is slightly shifted toward polarons. As discussed in section III.A, an increased concentration of doped polymer leads to a more ionic medium where counterions are less strongly bound to the charged polycation. When ionic separation occurs (to a polyelectrolyte), the effective Coulomb repulsion between charges in a bipolaron is increased. Taken to the extreme, this ionic self-screening of the doped polymer can lead to a destabilization of the bipolaron with respect to two polarons. Evidently, the energy difference between polarons and bipolarons does change with polymer concentration. Although bipolarons remain the dominant charge-storage state even at $c > c_0$, the increase in effective Coulomb interaction must be sufficiently large to account for the observed rise in the polaron population.

A possible test of these ideas was to redo these experiments in a more polar solvent such as methylene chloride (the principal subject of this paper). One would expect, in this case, that the solvent would more strongly solvate any charged states on the polymer chains and, hence, any effect neighboring doped chains might have would be minimized. Indeed, there is no polymer concentration dependence exhibited in either the magnetic or optical data of the methylene chloride solutions at a fixed doping level. The doping data are also in agreement. The spin-to-charge ratio indicates that charge is predominantly stored in polarons at low doping levels. Evidently, the on-chain

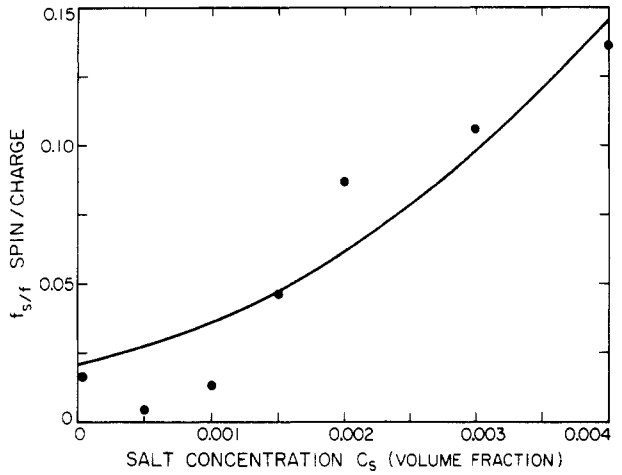

Figure 9. Magnetic susceptibility versus concentration of added salt solution of tetrabutylammonium perchlorate at a fixed polymer concentration, $c = 0.1c_0$, and fixed dopant level, $y = 2\%$, in chloroform. A 0.1 M salt concentration is equivalent to a volume fraction of 2×10^{-3} on the abcissa. The ordinate is the spin to charge ration f_s/f.

Coulomb repulsion term has been sufficiently raised (by removal/screening of the counterions) that (Δ/kT) is smaller for P3HT in methylene chloride than in chloroform. Statistical considerations (entropy) can then cause a shift of the equilibrium toward polaron formation at low doping levels and at room temperature. Only at higher doping levels does one see a majority of bipolarons, in agreement with the results of the statistical models developed in the previous section. This competition of entropy and energy is not important for experiments carried out at low temperatures. For experiments at the moderately low temperature of 100 K, for example, (Δ/kT) will be three times larger than at room temperature, leading to a larger η by a factor of 10^5 and a polaron population at least a factor of 100 less. Consequently, entropic considerations are not expected to play a role in low-temperature measurements, such as in the photoinduced studies of polythiophene,[7] where they are too weak to effect the energetically favored bipolaron population.

A classic test of ideals such as (doped) polymer–polymer ionic screening leading to polyelectrolyte behavior is to prepare the system in its nonpolar, noninteracting (dilute polymer concentration) state and to introduce a completely different ionic species to see if the screening effect still exists. This was precisely done in a series of experiments by adding salt (tetrabutylammonium perchlorate) to a P3HT solution in chloroform at low polymer concentration ($c = 0.1c_0$) and at a low doping level ($y = 2\%$). Without salt, one observes few spins (spin/charge = 1/80) so that most of the charge is stored in bipolarons. As one adds more and more tetrabutylammonium perchlorate to the solution, the spin signal grows dramatically. At higher salt concentrations, the spin to charge ratio has increased to 1/8 (Figure 9), indicating a controlled increase in the number of polarons by an order to magnitude! We conclude that ionic self-screening is a useful concept in understanding the magnetic and optical properties of doped conducting polymers in solution and consider this in more detail in the following section.

V.B. The Hubbard Lattice Gas Model. In an effort to understand in greater detail how ionic screening can lead to behavior such as observed in Figure 9, we have studied a Hubbard lattice gas model.[19,20] Given a lattice of L sites, ν chains, N monomers per chain, and n dopants (and, hence, counterions) per chain, one can write as dimensionless volume fraction the concentration of monomers as $c = N\nu/L$ and the concentration of dopants as $c_d = n\nu/L$. The solution has a characteristic Debye screening length, κ, where κ^2 is proportional to the concentration of counterions plus the concentration of salt: $\kappa^2 = (\text{constant})(c_{salt} + c_d)$. Let ϵkT be the binding energy of a counterion to its coion:

$$\epsilon = \epsilon_0 e^{-\kappa a} \tag{32}$$

where Debye screening is assumed to be operative on the binding between counterion and coion. Let UkT be the binding energy of two neutral polarons to form a bipolaron. In this nomenclature, a neutral polaron is a polaron with its bound counterion. Therefore, the number of neutral polarons is the number of associated counterions, while the number of charged polarons is the number of dissociated counterions. Charged bipolarons (i.e., with one or more counterions missing) are excluded on energetic grounds.

To calculate the statistical properties of this system, one needs to write down the partition functions for the polymer and solvent. Given $L - N\nu$ solvent sites and a counterion chemical potential of μ_c, the solvent site partition function is

$$z_s = 1 + e^{\mu_c} = 1 + x_c \tag{33}$$

where x_c is a shorthand notation and β is set equal to one for convenience. The grand partition function is then $Z_s = z_s^{L-N\nu}$. Likewise, given the polaron chemical potential, μ_p, and examining the possible states of a polymer site (empty, charged polaron, neutral polaron, or neutral bipolaron), we can write

$$z_p = 1 + e^{\mu_p} + e^{\mu_p+\mu_c-\epsilon} + e^{2(\mu_p+\mu_c-\epsilon)-U} = 1 + x_p + x_p\tilde{x}_c + x_p^2\tilde{x}_c^2 y \tag{34}$$

where we define $x_p = \exp(\mu_p)$. The ionic screening dependence is contained in the quantity $t = e^{\epsilon}$, $\tilde{x}_c/t = \exp(\mu_c)$, and $y = e^{-U}$. The grand partition function of the polymer is $Z_p = z_p^{N\nu}$ and for the entire system $Z = Z_p Z_s$.

The total number of dopants is the total number of counterions, i.e., the number of bound counterions plus the number of dissociated counterions. The counterion chemical potential allows us to write this statement as

$$c_d = \frac{1}{z_p}\frac{\partial z_p}{\partial \mu_c}c + (1-c)\frac{1}{z_s}\frac{\partial z_s}{\partial \mu_c} \tag{35}$$

where we have divided the number of species by L to get concentrations. Similarly, the polaron chemical potential allows us to write another expression for c_d:

$$c_d = \frac{1}{z_p}\frac{\partial z_p}{\partial \mu_p}c \tag{36}$$

Furthermore, if one calculates the concentration of bipolarons

$$c_b = \frac{1}{z_p}\frac{\partial z_p}{\partial U}c \tag{37}$$

then charge conservation leads to the concentration of polarons

$$c_p = c_d - 2c_b \tag{38}$$

Carrying out the calculation, eq 35 yields

$$c_d = \frac{x_p\tilde{x}_c + 2x_p^2\tilde{x}_c^2 y}{z_p}c + (1-c)\frac{x_c}{1+x_c} \tag{39}$$

and

$$f = \frac{c_d}{c} = \frac{x_p + x_p\tilde{x}_c + 2x_p^2\tilde{x}_c^2 y}{z_p} \tag{40}$$

Note that f is in fact the doping level of the polymer. Combining eq 39 and 40 yields the simple expression

$$\frac{c}{1-c} = \frac{z_p}{x_p}\frac{x_c}{1+x_c} \tag{41}$$

which together with eq 34 and 40 allows us to derive the appropriate ranges for the critical parameters y (or U) and $\tilde{x}$ (or t, which contains the Debye length).

An expression for the polaron concentration as a function of salt or polymer concentration can be derived from eq 34, 37, and 38, yielding

$$f_s = f - 2x_p^2\tilde{x}_c^2 y/z_p \tag{42}$$

where $f_s = c_p/c$, or the number of polarons per monomer unit. To write this expression in terms of the desired parameters and known variables, we substitute the expression for z_p from eq 34 into eq 40, and we solve the quadratic equation for x_p exactly. To derive the correct limiting expression, one must be in the right ranges of the parameters and limits of the equations. Calculation of the nominal polymer concentration yields a dimensionless volume fraction of $c \sim 10^{-5}$–10^{-4}. From careful analysis of eq 41, this implies that x_c must be at least as small. Since a reasonable regime for t is 10^2–10^4, one can conclude $\tilde{x}_c < 1$. Given a doping level of $f = 0.02$ for the salt concentration data of Figure 9 and assuming a large y, the quadratic equation can be reduced to

$$x_p = \frac{-1 + (1 + 8fy\tilde{x}_c^2)^{1/2}}{4\tilde{x}_c^2 y} \tag{43}$$

Making the reasonable assumption that $8fy\tilde{x}_c^2 \gg 1$, we further simplify eq 43. In this limit, we also find $x_c \approx cx_p$. Finally, the expression for the spin (polaron) concentration of eq 43 can be written only in terms of the adjustable parameters y and t (f and c fixed):

$$f_s = \frac{f^2}{2}\left[1 + \left(\frac{8}{yf^1c^2t^2}\right)^{1/4}\right] \tag{44}$$

Recall y is the exponential of U, the binding energy for a bipolaron. Likewise, t represents the binding energy of a counterion to a polaron and contains all the salt concentration dependence and some monomer concentration dependence in an exponential of an exponential. The calculated polymer concentration is at least an order of magnitude less than that of the salt and is hence neglected. The solid line in Figure 9 is the best fit to eq 44 and yields approximately 0.40 eV for both binding energies. Although this energy is too high to be accurate, it is certainly in the right range. If there is no salt added to the solution, the polymer concentration dependence becomes important in the exponential. Unfortunately, this functional form was unable to reproduce the dramatic polymer concentration behavior reported by Nowak et al.[9a] and shown in Figure 10. This suggests that the doped polymer interchain interaction is of a more complex nature than a simple ionic screening theory can accommodate. More work is necessary to elucidate the nature of the interchain interaction in a concentrated solution of doped conducting polymers.

VI. Conclusion

The small difference in energy of the charge storage configurations in a doped soluble conducting polymer in solution provides an opportunity to control the magnetic and optical properties of the polymer. Specifically for P3HT, to have significant numbers of polarons, it is best to dissolve and lightly dope the polymer in more polar solvents such as CH_2Cl_2. Otherwise, in less polar solvents such as $CHCl_3$, a small equilibrium population of polarons can exist by having high polymer concentrations or by simply adding salt. Nevertheless, bipolarons are the energetically more stable species and dominate the optical and magnetic data in most cases, specifically in nonpolar solvents or in more polar solvents with the polymer doped to a high doping level.

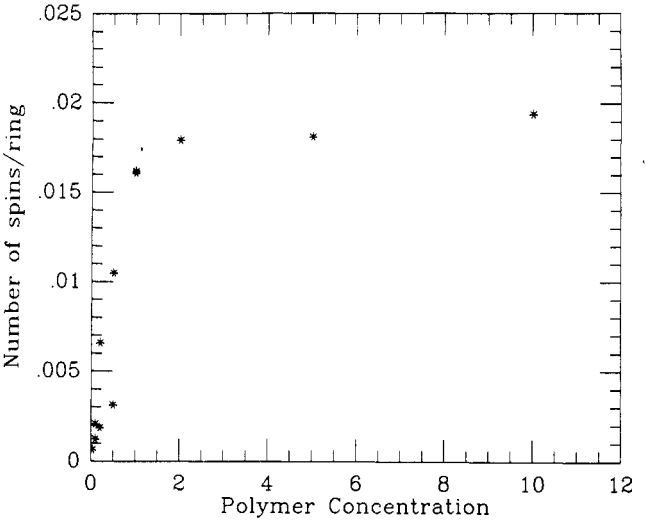

Figure 10. Number of spins per thiophene ring as a function of doped polymer concentration (in chloroform) at a fixed dopant level ($y = 0.08$). The polymer concentration is given in units of c_0, where $c_0 \approx 6 \times 10^{-3}$ M.

From the results presented in this and earlier studies[8,9,15,16] of doped conducting polymers in solution, we conclude that the concepts developed in studying the one-dimensional conductors in the solid state are readily applicable to conducting polymers in solution whether isolated or in the semidilute regime. In solution, the screening due to either foreign ions or to neighboring doped polymers can enhance the effective electron–electron Coulomb repulsion enough to allow the statistical mechanics of the system to favor a dominant equilibrium population of polarons over its energetically more stable bound state, the bipolaron.

Statistical considerations become important in understanding the dynamics of charge storage in P3HT in solution precisely because this system allows entropy to become important; i.e., the polymers are free to sample a much greater configurational space in solution than in the solid state. This is substantiated by previous experimental results together with this work. Solid-state data have failed to produce conclusive optical or magnetic signatures of polarons. On the contrary, since the data are in agreement with what is expected for bipolarons, it has been concluded that bipolarons are energetically favored. With the polymer in solution, a number of possible interactions (as well as the configurational entropy) can change the relative energy between polarons and bipolarons. We find that bipolarons are still the more stable species; however, the difference in energies is sufficiently reduced to allow entropy to play an important role. Hence, for the first time, we see optical and magnetic signatures (at low doping levels in a polar solvent) that can reasonably be assigned to polarons.

Acknowledgment. The electron spin resonance studies were supported by NSF DMR85-21392. The optical and IR studies in solution were supported by NSF DMR86-15483. We thank Professor J.-L. Bredas for important comments on the assignment of the polaron infrared ab-

sorption spectral features and for carefully reading the manuscript.

Registry No. P3HT, 108568-44-1; $NO^+PF_6^-$, 16921-91-8; tetrabutylammonium perchlorate, 1923-70-2.

References and Notes

(1) (a) Heeger, A. J.; Kivelson, S.; Schrieffer, J. R.; Su, W.-P. *Rev. Mod. Phys.*, in press. (b) *Handbook of Conducting Polymers*; Skotheim, T. J., Ed.; Marcel Dekker: New York, 1986. (c) Etemad, S.; Heeger, A. J.; MacDiarmid, A. G. *Annu. Rev. Phys. Chem.* **1982**, *33*, 443. (d) Bredas, J.-L.; Street, G. B. *Acc. Chem. Res.* **1985**, *18*, 309.

(2) (a) Su, W.-P.; Schrieffer, J. R.; Heeger, A. J. *Phys. Rev. Lett.* **1979**, *42*, 1698; *Phys. Rev. B* **1980**, *22*, 2099. (b) Rice, M. J. *Phys. Lett. A* **1979**, *71A*, 152. (c) Takayama, H.; Lin-Liu, Y. R.; Maki, K. *Phys. Rev. B* **1980**, *21*, 2388.

(3) (a) Brazovskii, S. A.; Kirova, N. *JETP Lett.* **1981**, *33*, 4. (b) Campbell, D. K.; Bishop, A. R. *Phys. Rev. B* **1981**, *24*, 4859; *Nucl. Phys. B* **1982**, *200*, 297.

(4) (a) Heeger, A. J. *Comments Solid State Physics* **1981**, *10*, 53. (b) Laughlan, L.; Etemad, S.; Chung, T.-C.; Heeger, A. J.; MacDiarmid, A. G. *Phys. Rev. B* **1981**, *29*, 3701.

(5) (a) Chung, T.-C.; Kaufman, J. H.; Heeger, A. J.; Wudl, F. *Phys. Rev. B* **1981**, *30*, 702. (b) Chen, J.; Heeger, A. J. *Solid State Commun.* **1986**, *58*, 251.

(6) (a) Schaffer, H.; Heeger, A. J. *Solid State Commun.* **1986**, *59*, 415. (b) Colaneri, N.; Nowak, M. J.; Spiegel, D.; Hotta, S.; Heeger, A. J. *Phys. Rev. B* **1987**, *36*, 7964.

(7) (a) Kim, Y. H.; Hotta, S.; Heeger, A. J. *Phys. Rev. B* **1987**, *36*, 7486. (b) Vardeny, Z.; Ehrenfreund, E.; Brafman, O.; Nowak, M. J.; Schaffer, H.; Heeger, A. J.; Wudl, F. *Phys. Rev. Lett.* **1986**, *56*, 671.

(8) Jen, K. Y.; Oboodi, R.; Elsenbaumer, R. L. *Polym. Mater. Sci. Eng.* **1985**, *53*, 79; *Synth. Met.* **1986**, *15*, 169.

(9) (a) Nowak, M. J.; Rughooputh, S. D. D. V.; Hotta, S.; Heeger, A. J. *Macromolecules* **1987**, *20*, 965. (b) Hotta, S.; Rughooputh, S. D. D. V.; Heeger, A. J.; Wudl, F. *Macromolecules* **1987**, *20*, 212. (c) Rughooputh, S. D. D. V.; Hotta, S.; Heeger, A. J.; Wudl, F. *J. Polym. Sci., Polym. Phys. Ed.* **1987**, *25*, 1071. (d) Rughooputh, S. D. D. V.; Nowak, M. J.; Hotta, S.; Heeger, A. J.; Wudl, F. *Synth. Met.* **1987**, *21*, 41. (e) Colaneri, N. PhD Thesis, University of California, Santa Barbara, unpublished.

(10) (a) Genoud, F.; Guglielmi, M.; Nechtschein, M.; Genies, E.; Salmon, M. *Phys. Rev. Lett.* **1985**, *55*, 118. (b) Nechtschein, M.; Devreux, F.; Genoud, F.; Vieil, E.; Pernaut, J.; Genies, E. *Synth. Met.* **1986**, *15*, 59. (c) Devreux, F.; Genoud, F.; Nechtschein, M.; Villerat, P. *Synth. Met.* **1987**, *18*, 89.

(11) Rughooputh, S. D. D. V. Unpublished results.

(12) Bredas, J.-L.; Wudl, F.; Heeger, A. J. *Solid State Commun.* **1987**, *63*, 577.

(13) Baeriswyl, D. Private communication.

(14) Pincus, P. A.; Rossi, G.; Cates, M. E. *Europhys. Lett.* **1987**, *4*, 41.

(15) Spiegel, D.; Pincus, P.; Heeger, A. J. *Polym. Commun.*, in press.

(16) Spiegel, D.; Heeger, A. J. *Polym. Commun.* **1988**, *29*, 266.

(17) Kaufman, J. H.; Chung, T.-C.; Heeger, A. J. *J. Electrochem. Soc.* **1984**, *131*, 2847.

(18) Stafstrom, S.; Bredas, J.-L. *Phys. Rev. B*, in press.

(19) Pincus, P.; Chaikin, P.; Coll, C. F., III. *Solid State Commun.* **1973**, *12*, 1265.

(20) Pincus, P. *Selected Topics in Physics, Astrophysics, and Biophysics*; D. Riedel: Dodrecht, Holland, 1973.

Graphical Method for Polymerization Kinetics. 3.† Living Polymerization with Nonequal Propagation Rate Constants

Deyue Yan

Department of Applied Chemistry, Shanghai Jiao Tong University, 1954 Hua Shan Road, Shanghai 200030, The People's Republic of China. *Received October 19, 1988*

ABSTRACT: According to Schulz et al., the propagation rate constants depend upon the degree of polymerization in the initial stage of the anionic polymerization of methyl methacrylate in tetrahydrofuran at −46 °C. This work deals with the non-steady-state kinetics for the living polymerizations with nonequal propagation rate constants, using the graphical technique. Several cases have been taken into account, and expressions for the number- and weight-average degrees of polymerization, the heterogeneity index, and the molecular weight distribution function are derived. The relationships between the reaction conditions and the molecular parameters of the resultant polymer have also been established.

Introduction

Terminationless polymerization was first described by Ziegler[1-3] and later by Mark.[4] For living polymerization with the initiation rate constant equal to the propagation constant, Flory[5] has given the Poisson distribution for the polymer formed. However, it was Szwarc[6,7] who actually discovered living polymerization in 1956 on the basis of highly convincing experiments. Two years later, Gold[8] took account of the fact that the rate constant of initiation is different from that of propagation and obtained the improved Poisson distribution. It is of interest that several authors[9-12] have estimated the individual propagation rate constants from their own experimental data. Maget[13] have studied theoretically the molecular weight distribution for living polymerization with n reaction steps and nonequal rate constants. However, the other important molecular parameters, such as the number- and weight-average degrees of polymerization and the heterogeneity index, have not yet been reported. Mita[14] has dealt with this problem with the assumptions of instantaneous initiation and m propagation steps, but little improvement has been made. Recently, Schulz and co-workers[12] have reported that the propagation rate constants vary with the degree of polymerization in the initial stage of the anionic polymerization of MMA in THF at −46 °C and compared the experimental results with numerical solutions of the related kinetic equations. Obviously, it is necessary to treat comprehensively living polymerization with nonequal propagation rate constants. Using the graphical method[15-17] and Laplace transformation, all the molecular parameters for the resulting living polymer are derived in this paper.

1. General Treatment

The differential equations for the formation and disappearance of the living n-mer N_1, N_2, ..., N_n, as well as for the consumption of initiator N_0, are given by the following equations:

† Part 2: cf. ref 17.

0024-9297/89/2222-2926$01.50/0 © 1989 American Chemical Society